Strain-Stabilized Solid Phase Epitaxy of Si–Ge on Si.

Strain-stabilized solid phase epitaxy of Si–Ge on Si

Jennifer F. Sage, William Barvosa-Carter,[a] and Michael J. Aziz
Division of Engineering and Applied Sciences, Harvard University, Cambridge, Massachusetts 02138

(Received 5 February 2006; accepted 28 March 2006; published online 14 June 2006)

We compare solid phase epitaxial growth of amorphous Si–Ge alloys created by Ge ion implantation into Si with and without the imposition of 0.5 GPa of externally applied biaxial tensile stress. External loading stabilizes the growth front against roughening, resulting in a doubling of the maximum reported Ge concentration for stable growth to 14 at. %. The externally applied stress appears to superpose with the intrinsic compositional stress and indicates a threshold of approximately 0.6 GPa for interface breakdown. This principle is expected to be applicable to expanding the composition range for stable growth of other semiconductor alloy combinations by other growth techniques. © *2006 American Institute of Physics*. [DOI: 10.1063/1.2200448]

I. INTRODUCTION

Band-gap engineering using compositionally or mechanically strained semiconductor layers has become a useful tool for device designers looking to extend the capabilities of Si-based semiconductor devices.[1] As a result, an increasing number of Si-based architectures involving strained layers are being investigated for use in photonic and high-speed electronic devices.[2] However, the strain introduced by the incorporation of Ge into the Si lattice can cause the formation of extended defects, and different fabrication techniques require different defect engineering approaches to reduce their impact. One technique for producing these alloys is ion implantation of Ge into a Si substrate and crystallization of the resulting amorphous surface layer by solid phase epitaxial growth (SPEG). This process has also been used to improve structural quality[3] and enhance dopant activation.[4] With this method, the strain caused by the lattice mismatch places an upper limit of 3–7 at. % on the amount of Ge that can be incorporated into the Si lattice before interfacial breakdown into a rough growth front occurs, causing the generation of defects, such as {111} facets and stacking faults, leading to severely degraded material not suitable for devices.[5–10]

We present an approach for increasing the amount of Ge that can be incorporated into the lattice during SPEG while still maintaining a smooth interface. As interface roughness leads to defects in the crystal, this approach is expected to yield a crystal with fewer extended defects.[5,8,9] This stress-anneal method utilizes external loading during growth to exert a tensile stress on the interface. The external tensile stress partially compensates for the intrinsic compositional stress present in heteroepitaxial growth and thereby allows material with a higher Ge concentration to be grown without interface breakdown.

II. EXPERIMENT

Si(001) wafers were implanted with 200 keV $^{74}Ge^{+}$ to a dose of either $6.5\times10^{16}/cm^2$ or $1.0\times10^{17}/cm^2$, producing a Ge profile with a peak concentration[11] of 10% or 15%, respectively, located at a depth of 115 nm, as shown in Fig. 1. The samples were then subjected to a second implant of $^{28}Si^{+}$ at 200 keV and 77 K to a dose of $2\times10^{15}/cm^2$. This second implant served to ensure complete amorphization of the top layer and move the initial amorphous/crystal (a/c) interface to a depth of approximately 300 nm, which is well beyond the tail of the Ge profile, without altering the Ge profile significantly. This ensured that the regrowth would begin in an area far from the chemical and elastic effects of the Ge, and that the end of range defects would be far from the Ge-bearing region.

Because wafers can be annealed under external loading for only a limited duration before fracturing,[12] all samples were preannealed without external loading on a hot stage in order to start the regrowth and move the interface nearer the peak of the Ge profile. The resulting interface depth varied among samples from 130 to 190 nm. The samples were then annealed for approximately 2 h at a temperature of 510 °C while subjected to a biaxial tensile stress of

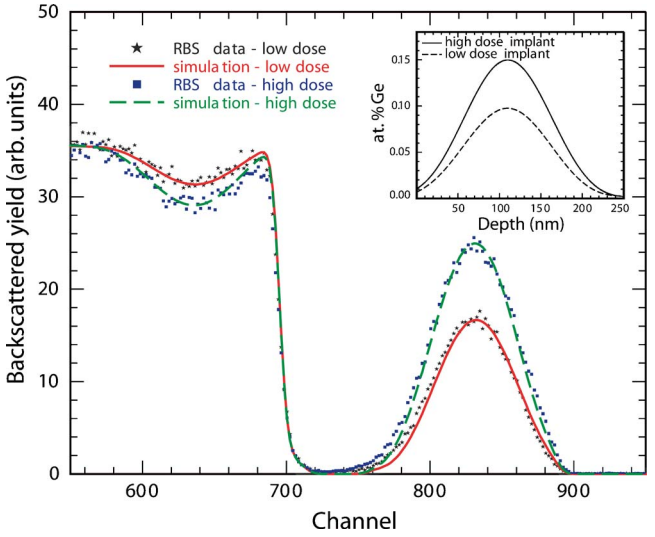

FIG. 1. (Color online) Grazing exit Rutherford backscattering spectrometry (RBS) data for low- and high-dose implants and simulated RBS spectra from calculated depth profile. Inset shows Ge concentration vs depth profile input into simulations.

[a]Present address: HRL Laboratories, LLC, Malibu, CA. Electronic mail: wbc@hrl.com

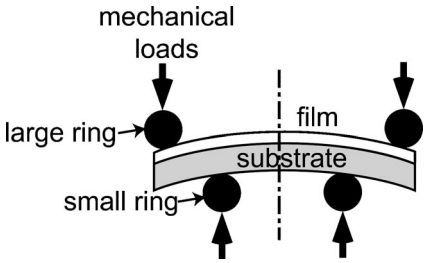

FIG. 2. Schematic of apparatus for external application of stress to growth front. Amorphous-crystal interface is subjected to biaxial tension by loading between two rings.

$\sigma_{biax} = +0.5$ GPa, using a stress-annealing apparatus described elsewhere[13] and shown schematically in Fig. 2. The resulting interface depth varied among samples from 97 to 146 nm. The samples were then cleaved into two pieces, and one piece was completely crystallized without external loading on a hot stage while the interface depth and growth velocity were studied in real time using *in situ* time-resolved reflectivity (TRR).[14] This technique permitted us to monitor the evolution of the interface roughness when samples were not loaded; note that due to the geometry of the loading apparatus, we did not obtain *in situ* TRR data while the samples were under load.[12] Cross-sectional transmission electron microscopy (XTEM) was used to observe

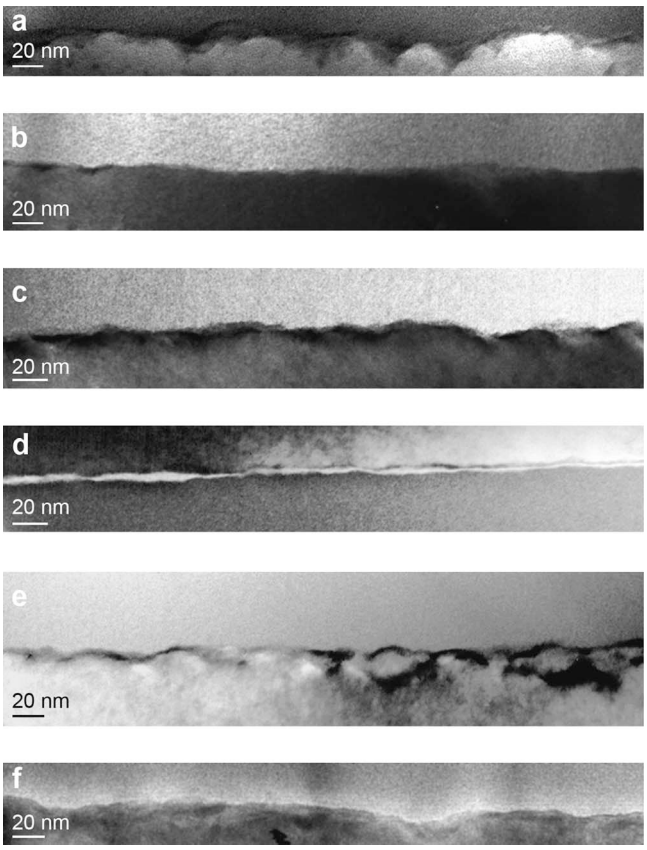

FIG. 3. Cross-section transmission electron micrographs of unstressed (a) and stressed (b) regions of sample 1 (low dose) when growth is stopped at depth of (a) 100 nm and (b) 97 nm. Unstressed (c) and stressed (d) regions of sample 2 (high dose) when growth is stopped at depth of (c) 146 nm and (d) 128 nm. Unstressed (e) and stressed (f) regions of sample 3 (high dose) when growth is stopped at depth of (e) 138 nm and (f) 113 nm.

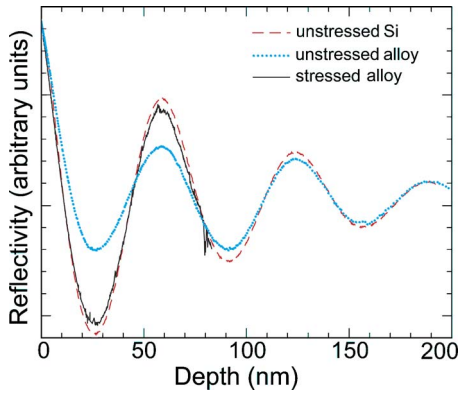

FIG. 4. (Color online) Time-resolved optical reflectivity of low-dose sample during growth. Time proceeds right to left, and the experiment is over when the depth reaches zero. Dashed line shows oscillations characteristic of pure Si with flat interface. Dotted line shows reduced amplitude during unstressed growth of SiGe. Degraded interface planarity reduces the amplitude of oscillation. Solid line shows smoother interface after stress has been applied from 130 to 97 nm.

the a/c interface of the piece that had not been fully crystallized on the hot stage. Control samples were obtained from the portions of the loaded samples that lay outside the load contacts (Fig. 2) or were made by crystallizing never-loaded samples entirely on a hot stage.

III. RESULTS

In Fig. 3 we compare XTEM images of the a/c interface for two regions of the same low-dose (10% peak) sample (sample 1) that have been subjected to the same thermal history. Figure 3(a) was taken from the outer portion of the sample (outside the loading rings) where the externally imposed stress was zero, whereas Fig. 3(b) was taken from a portion annealed while under an externally applied biaxial tensile stress of +0.5 GPa. The interface depth is 100 nm in Fig. 3(a) and 97 nm in Fig. 3(b) due to a higher growth rate for the material under tension.[15] In both cases the interface has just traversed the peak of the Ge concentration profile. It is apparent from the XTEM images that the externally loaded ("stressed") region of the sample exhibits a much smoother interface than does the region not loaded ("unstressed"). Smoother interfaces are less likely to develop regions with {111} orientations from which stacking faults can more readily nucleate.[9]

In Fig. 4 we compare the TRR trace for the stressed region of this sample [Fig. 3(b)] with a trace from an identically implanted piece of material that was annealed on a hot stage without external loading. Also shown are the oscillations expected (and seen in practice) from pure Si with a flat interface. The decreased amplitude of the TRR signal of the sample annealed without external loading is indicative of a rough a/c interface.[12] The sample annealed under loading during growth through the peak of the Ge profile and subsequently annealed without loading for investigation with TRR shows an amplitude that, while slightly less that of the pure Si case, is much greater than that of the unloaded sample, indicating that the stress-anneal technique maintains a much smoother interface than that without external loading, even after stress annealing for just part of the growth.

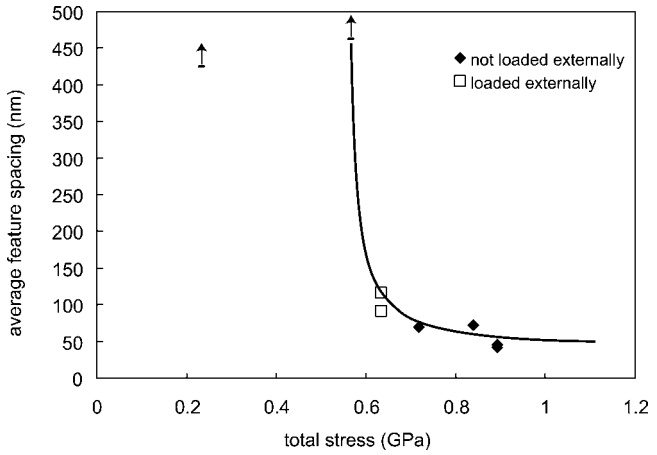

FIG. 5. Average spacing of V-shaped features from XTEM vs "total" stress, assuming a linear superposition of externally applied and compositional stresses. The two points above 400 nm are merely lower limits based on the limited region of observation of stressed samples in XTEM. The results are consistent with a single curve, drawn as a guide to the eye.

In Figs. 3(c)–3(f) we show corresponding XTEM images for two different high-dose (15% peak) samples. Sample 2 [Figs. 3(c) and 3(d)] was preannealed without external loading to an interface depth of approximately 190 nm. After annealing under load, the unstressed region shown in Fig. 3(c) has an interface depth of 146 nm and the stressed region shown in Fig. 3(d) has an interface depth of 128 nm. In comparison with Fig. 3(c), Fig. 3(d) shows that while the interface in the stressed region did not quite reach the peak of the Ge profile, the use of this external loading technique permitted the propagation of a smooth interface up to a local Ge concentration of 14%.

Sample 3 [Figs. 3(e) and 3(f)] was preannealed without external loading to an interface depth of 160 nm. After annealing in the loading apparatus, the unstressed region shown in Fig. 3(e) has an interface depth of 138 nm and the stressed region shown in Fig. 3(f) has an interface depth of 113 nm. The interface in the stressed region of this sample is at the peak of the Ge profile, which is the location of maximum compositional stress. XTEM images in Fig. 3 indicate that while the interface in the stressed material still exhibits some roughness, the characteristic wavelength of the roughness in Fig. 3(f) is much less than that in Fig. 3(e), which is consistent with previous observations on compressively loaded material.[12] A longer wavelength at the same amplitude implies a reduced average misorientation from (001) and a correspondingly reduced probability of extended defect generation. It is also worth noting that in the absence of external loading, the interface roughness in SPEG of Ge-implanted Si increases with Ge concentration[5,12] and the roughness is therefore expected to be maximized at the position of Fig. 3(f). Thus the stressed material in Fig. 3(f) illustrates an improved interface configuration over that of the unstressed material in Fig. 3(e) despite the higher compositional stress.

TABLE I. Maximum Ge concentration incorporated into crystal by Ge implantation and SPEG.

Max. Ge% at interface	Roughness observed	External loading	Implant energy (keV)	Study
3	No		80	Zeng *et al.*[a]
6.4	Yes		25,40,100[b]	Corni *et al.*[c]
4	No		70	Cristiano *et al.*[d]
11	Yes		70	Cristiano *et al.*[d]
7	No		140	Cristiano *et al.*[d]
3	No		200	Howard *et al.*[e]
7	No		200	Howard *et al.*[e]
10	Yes		200	Sample 1, not loaded
10	No	X	200	Sample 1, loaded
12	Yes		200	Sample 2, not loaded
13	Yes		200	Sample 3, not loaded
13	Yes		200	Howard *et al.*[e]
14	Yes		200	Paine *et al.*[f]
14	No	X	200	Sample 2, loaded
15	Yes[g]	X	200	Sample 3, loaded
24	Yes		200	Cristiano *et al.*[d]
2	No		400	Cristiano *et al.*[d]
5	No		400	Cristiano *et al.*[d]
6	Yes		400	Cristiano *et al.*[d]
8	Yes		400	Cristiano *et al.*[d]
21	Yes		800	Elliman and Wong[h]
34	Yes		800	Elliman and Wong[i]

[a]Reference 10.
[b]All three implants on the same sample.
[c]Reference 17.
[d]Reference 18.
[e]Reference 8.
[f]Reference 9.
[g]This sample showed some roughness, but the interface was smoother than the sample that contained 13% Ge.
[h]Reference 6.
[i]Reference 5.

TRR results for samples 2 and 3 are similar to that for sample 1. The amplitude of the reflected signal after stressed growth is between that for the same region in unstressed growth and that for unstressed pure Si, indicating that the roughness for the stressed material is not as great as for unstressed alloy material but greater than for unstressed, pure Si.

IV. DISCUSSION

A relevant question is whether the externally applied and compositional stresses superpose and offset each other directly, or whether the interaction is more complicated. If linear elasticity is used to calculate the compositional stress as a function of the depth-dependent Ge concentration, and the externally applied stress is assumed to add directly to the compositional stress, then the "total" stress as a function of depth can be determined. The average spacing of the V-shaped features observable in XTEM is plotted in Fig. 5 versus this total stress. The estimated uncertainty in spacing evaluated by this method is about a factor of 2. The results are describable by a single curve, indicating that as far as we can tell at this time, the stresses simply superpose to create a threshold of approximately 0.6 GPa total stress.

This technique is successful in enabling defect-free growth at higher alloy compositions because the temperature required for measurable SPEG is below the ductile-brittle transition temperature of the Si substrate.[16] However, it is important to note that, while plastic flow of the substrate is dramatically inhibited, some permanent deformation does occur around stress concentrations (e.g., the contact points on the loading apparatus). Such deformation leads to failure of the sample, thereby limiting the total amount of regrowth that can be accomplished. Hence, thinner layers should be easier to crystallize completely.

In Table I we compare our results with previous works. Our results should be most directly comparable to the other studies of 200 keV implants. Howard *et al.*[8] examined samples with 200 keV implant doses of $1.8\times10^{16}/\mathrm{cm}^2$, $3.6\times10^{16}/\mathrm{cm}^2$, and $5.3\times10^{16}/\mathrm{cm}^2$, corresponding to peak Ge concentrations of 3%, 7%, and 13%. TEM showed the interfaces for the lower two implant doses to be featureless, but the 13% Ge sample had a highly defected microstructure showing both {111} facets and stacking faults. Paine *et al.*[9] implanted one set of samples at 200 keV to a dose of $9.6\times10^{16}/\mathrm{cm}^2$ for a peak Ge concentration of 14%. TEM of this sample after partial regrowth showed an uneven interface with V-shaped features and {111} facets and an estimated interface width of 40 nm. Our samples without external loading behave in a very similar fashion, showing some degree of interface roughening down to the lowest Ge concentration investigated of 10%. Our results for the low-dose sample 1 show that the stress-anneal technique results in a very smooth interface for a sample with 10% Ge, which exceeds the highest concentration, 7%, that had previously been incorporated. The results for the high-dose sample 2, which was not grown all the way to the concentration peak, demonstrate that the stress-anneal technique results in a smooth surface when the local Ge concentration at the interface is 14%, even though a concentration of 12% causes roughness in the unstrained material. The results for the high-dose sample 3, which was grown virtually all the way to the concentration peak, show that although 13% Ge causes a great deal of roughness without external loading, the stress-anneal technique results in material with 15% Ge with a superior interface configuration.

V. SUMMARY

We have demonstrated the viability of a strain-stabilized heteroepitaxial growth technique for growing defect-free SiGe alloy layers with a higher Ge concentration than was previously attainable by SPEG. With the external application of a biaxial tensile stress in the plane of the a/c interface during SPEG, the a/c interface is stabilized against roughening, thereby reducing the likelihood of faulted growth and leading to a strained alloy film more suited for device fabrication. We expect that this method can also be used to expand the composition range for stable growth of other semiconductor alloy combinations by any growth technique that can be performed at temperatures below the ductile-brittle transition.

ACKNOWLEDGMENTS

The authors acknowledge Cheng-Yen Wen for help with XTEM. This research was supported NSF-DMR-0213373 and NSF-DMR-9813803.

[1] S. L. Wu, Y. M. Lin, S. J. Chang, S. C. Lu, P. S. Chen, and C. W. Liu, IEEE Electron Device Lett. **27**, 46 (2006).
[2] T. Yin, A. M. Pappu, and A. B. Apsel, IEEE Photon. Technol. Lett. **18**, 55 (2006).
[3] Q. Xiao and H. Tu, J. Cryst. Growth **271**, 368 (2004).
[4] F. Cristiano, N. Cherkashin, P. Calvo, Y. Lamrani, X. Hebras, A. Claverie, W. Lerch, and S. Paul, Mater. Sci. Eng., B **114–115**, 174 (2004).
[5] R. G. Elliman and W. C. Wong, Appl. Phys. Lett. **69**, 2677 (1996).
[6] R. G. Elliman and W. C. Wong, Nucl. Instrum. Methods Phys. Res. B **80–81**, 678 (1993).
[7] R. G. Elliman, W.-C. Wong, and P. Kringhøj, Mater. Res. Soc. Symp. Proc. **321**, 375 (1994).
[8] D. J. Howard, D. C. Paine, and N. G. Stoffel, Mater. Res. Soc. Symp. Proc. **201**, 247 (1991).
[9] D. C. Paine, D. J. Howard, N. G. Stoffel, and J. A. Horton, J. Mater. Res. **5**, 1023 (1990).
[10] X. Zeng, T.-C. Lee, J. Silcox, and M. O. Thompson, Mater. Res. Soc. Symp. Proc. **321**, 503 (1994).
[11] All concentrations are reported here in units of at. %.
[12] W. Barvosa-Carter, M. J. Aziz, A. V. Phan, T. Kaplan, and L. J. Gray, J. Appl. Phys. **96**, 5462 (2004).
[13] J. F. Sage, W. Barvosa-Carter, and M. J. Aziz, Appl. Phys. Lett. **77**, 516 (2000).
[14] J. A. Roth, G. L. Olson, D. C. Jacobson, and J. M. Poate, Appl. Phys. Lett. **57**, 1340 (1990).
[15] M. J. Aziz, P. C. Sabin, and G.-Q. Lu, Phys. Rev. B **44**, 9812 (1991).
[16] J. Samuels and S. G. Roberts, Proc. R. Soc. London, Ser. A **421**, 1 (1989).
[17] F. Corni, S. Frabboni, R. Tonini, G. Ottaviani, and G. Queirolo, J. Appl. Phys. **79**, 3528 (1996).
[18] F. Cristiano, A. Nejim, Y. Suprun-Belevich, A. Claverie, and P. L. F. Hemment, Nucl. Instrum. Methods Phys. Res. B **147**, 35 (1999).